ANRIL: A Regulator of VEGF in Diabetic Retinopathy

Anu Alice Thomas, Biao Feng, and Subrata Chakrabarti

Department of Pathology and Laboratory Medicine, Western University, London, Ontario, Canada

Correspondence: Subrata Chakrabarti, Department of Pathology and Laboratory Medicine, Western University, London, Ontario N6A 5C1, Canada;
subrata.chakrabarti@lhsc.on.ca.

Submitted: August 19, 2016
Accepted: December 19, 2016

Citation: Thomas AA, Feng B, Chakrabarti S. ANRIL: a regulator of VEGF in diabetic retinopathy. *Invest Ophthalmol Vis Sci*. 2017;58:470–480. DOI: 10.1167/iovs.16-20569

Purpose. Long noncoding RNAs (lncRNAs) previously thought to be "dark matter" of the genome, play key roles in various biological processes. The lncRNA ANRIL is located at a genetic susceptibility locus for coronary artery diseases and type 2 diabetes. We examined the role of ANRIL in diabetic retinopathy, through study of its regulation of VEGF both in vitro and in vivo.

Methods. Human retinal endothelial cells (HRECs) were subjected to incubation in high glucose to mimic diabetes. ANRIL expression was measured with or without small interfering RNA (siRNA) knockdown in HRECs. ANRIL knockout mice, with or without streptozotocin-induced diabetes, were also investigated. Cell and tissues were measured for VEGF mRNA and protein expression. Functional alterations in VEGF were determined through tube formation, cell proliferation, and retinal vascular permeability assays. Vascular endothelial growth factor regulation through ANRIL's interactions with polycomb repressive complex 2 (PRC2) components and p300 were studied thorough PRC2 blocker, siRNA, and RNA immunoprecipitation (RNA-IP) assays.

Results. High glucose and diabetes caused ANRIL upregulation in HRECs and in the retina. Glucose-mediated elevation of ANRIL, on silencing, prevented VEGF expression. Such regulation involved ANRIL-mediated control of the PRC2 components p300 and miR200b. Direct binding of ANRIL to p300 and enhancer of zeste homolog 2 (EZH2; a PRC2 component) were elevated following exposure to high glucose levels.

Conclusions. Our results demonstrate for the first time that ANRIL regulates VEGF expression and function in diabetic retinopathy. This regulation is mediated by p300, miR200b, and EZH2 of the PRC2 complex.

Keywords: ANRIL, VEGF, angiogenesis, diabetic retinopathy, p300, EZH2

Diabetic retinopathy is the most common cause of blindness in individuals greater than 50 years of age, affecting one in three persons with diabetes.[1] It is a chronic vascular complication characterized by low-grade inflammation, serum leakage through microvasculature, loss of capillaries, increased vascular permeability, and eventually neovascularization.[2,3] The last decade has seen scientific and medical progress on early diagnosis and prevention to combat this condition. However, in this complication, a variety of defects lead to functional and structural alterations in the retina that remain a significant challenge.[4]

Endothelial cells (ECs), the main target of hyperglycemic damage, undergo growth, increased permeability, remodeling, and phenotypic alterations in diabetes.[5] Various vasoactive factors are involved in angiogenesis as seen in diabetic retinopathy. However, VEGF signaling in ECs represents a major rate-limiting step in this process.[6] Induced in response to increased oxidative stress, VEGF binds to and activates tyrosine kinase receptors VEGFR-1 and VEGFR-2. Production of VEGF may, however, be regulated at transcriptional and posttranscriptional levels.[7–10]

Transcriptional regulation in mammalian systems is critically characterized by dynamic switching between "active" and "inactive" states of chromatin in response to extracellular and intrinsic signals. Such signals include histone and DNA modifications as major epigenetic mediators, recently joined by several RNA molecules including microRNAs (miRNAs) and long noncoding RNAs (lncRNAs).[11,12] Advances in DNA/RNA sequencing techniques have highlighted the existence of numerous noncoding RNA (ncRNA) molecules with significant regulatory roles, impacting both physiology and diseases.[13–16] In particular, lncRNAs have been shown to be of importance in various biological process such as transcription, translation, splicing, and intracellular/extracellular trafficking.[17] Recent studies have identified large- and small-scale mutations affecting noncoding genomes. Mutations in lncRNAs have been linked to diseases such as cancers, neurodegenerative diseases, and genetic disorders.[18–23]

A recent genome-wide study revealed the existence of lncRNA ANRIL (antisense RNA to *INK4* locus). ANRIL has been noted to be significant in cardiovascular diseases, type 2 diabetes, glaucoma, intracranial aneurysm, and cancers.[24–28] ANRIL consists of 19 exons, spanning 126.3 kb and producing a 3.8-bp RNA. It is situated in the p15/CDKN2B-p16/CDKN2A-p14/ARF gene cluster.[29] ANRIL may have direct transcriptional effects or an indirect role as a recruiter of chromatin remodeling complexes like polycomb repressor complex 2 (PRC2) to specific genomic loci.[30,31] Overexpression of ANRIL has also been shown to regulate the histone acetylator p300.[32] Its role in epigenetic silencing of specific miRNAs has also been reported.[33]

We and others have previously shown that VEGF and other vasoactive factors are regulated at the transcriptional level through p300 and specific miRNAs.[34–36] We have also shown

Investigative Ophthalmology & Visual Science

that, in diabetic retinopathy, microRNA 200b (miR200b) regulates production of VEGF directly or through regulation of p300 and/or through PRC2 complex.[8,9] ANRIL may work though PRC2 complex and in other systems has been shown to have a regulatory role on p300.[31,32] Here, we examined the role of ANRIL in regulating VEGF production, its molecular mechanism, and action in diabetic retinopathy. These phenomena were studied in human retinal endothelial cells (HRECs) exposed to various levels of glucose, as well as in retinal tissues of diabetic mice. We further investigated whether ANRIL facilitates such effects by regulating miR200b in concert with the PRC2 complex and p300.

Methods

All reagents were obtained from Sigma (Oakville, ON, Canada) unless otherwise specified.

Cells

We used HRECs (Olaf Pharmaceuticals, Worcester, MA, USA) grown in endothelial basal media-2 (EBM-2) and supplemented with 10% fetal bovine serum. The cells were plated at a density of 4.3×10^5 cells/mL. Following 24-hour incubation in serum-free media (EBM-2), cells were incubated with various levels of D-glucose (5 mM/L, normal glucose [NG]; 25 mM/L, high glucose [HG] or 25 mM/L L-glucose, osmotic control [LG]) at 75% cell confluency as previously described.[37] 3-Deazaneplanocin A (DZNEP) pretreatment was also carried out where needed.[9] Each experiment was performed at least in triplicate.

siRNA Transfection

Human retinal endothelial cells were transfected with Lincode Human CDKN2B-AS1 siRNA (5 nmol/L; Dharmacon, Chicago, IL, USA) or silencer siRNA CDKN2B-AS (5 nmol/L; Ambion, Austin, TX, USA) using Lipofectamine2000 (Invitrogen, Burlington, ON, Canada). Scrambled controls were used. The cells were transfected for 3 hours and recovered in full media overnight. Cells were then incubated in media with various glucose levels as previously described by us.[9] Gene knockdown was verified by real-time RT-PCR, which showed ≈70% reduction of ANRIL expression (compared with scrambled control).

Animals

All procedures were conducted in accordance with the ARVO Statement for the Use of Animals in Ophthalmic and Vision Research. All animals were cared for according to the guiding principles in the care and use of animals. Western University and Animal Care and Veterinary Services approved the experiments. All experiments conform to the guide for care and use of laboratory animals published by the National Insitutes of Health (NIH Publication 85-23, revised in 1996).

ANRIL knockout (KO) mice with a 70-kb deletion on chromosome 4 (129S6/SvEvTac-Del[4C4-C5]1Lap/Mmcd), corresponding to the 58-kb interval on chromosome 9p21 in humans, were used.[38] The ANRILKO mice were obtained from Mutant Mouse Resource & Research Centre (MMRC, Davis, CA, USA) and administered five doses of streptozotocin (STZ) intraperitoneally (50 mg/kg in citrate buffer, pH 5.6) on alternate days. Age- and sex-matched littermate controls received identical volume of citrate buffer. Diabetes was confirmed by measuring blood glucose (>20 mmol/L) from a tail vein using a glucometer. Animals were monitored for changes in body weight and blood glucose. After 8 weeks of diabetes, mice were euthanized, and tissues were collected.

Microarray

For lncRNA microarray analysis, HRECs were incubated with various levels of glucose. Cellular RNA was extracted using RNA isolation kit (Ambion, Carlsbad, CA, USA). Custom analysis of lncRNA expression profiling was performed by Arraystar, Inc. (Rockville, MD, USA).

RNA Analysis

RNA was extracted with TRIzol reagent (Invitrogen, Carlsbad, CA, USA) as previously described.[37] Complementary DNA for PCR was synthesized using high-capacity cDNA reverse-transcription kit (Applied Biosystems, Burlington, ON, Canada). Real-time RT-PCR to detect mRNA expression was done in the LightCycler (Roche Diagnostics, Mississauga, ON, Canada). Housekeeping gene β-actin mRNA was used to normalize the data.

microRNA Analysis

microRNA was isolated using mirVANA miRNA isolation kit (Ambion, Austin, TX, USA).[8,34,37] Complementary DNA for PCR was synthesized with high-capacity cDNA reverse-transcription kit (Applied Biosystems). Real-time RT-PCR was performed with TaqMan miRNA Assays (Applied Biosystems) in a LightCycler (Roche Diagnostics). miR-200b expression levels were normalized to housekeeping gene U6.

Enzyme-Linked Immunosorbent Assay

An ELISA was performed to measure the expression of VEGF protein using a commercially available kit (ALPCO, Salem, NH, USA; R&D Systems, Minneapolis, MN, USA) according to the manufacturer's instructions.[34]

Tube Formation Assay

Human retinal endothelial cells (1.5×10^4/well) were seeded on BD Phenol Red-Free Matrigel matrix (100 μL/well; BD Biosciences, Bedford, MA, USA) into a 96-well plate. After 1-hour incubation at 37°C, growth medium was replaced with serum-free medium containing appropriate amounts of glucose.[9] Recovery experiments were performed by incubating treated cells with VEGF (20 ng/mL). Pictures were taken at 40× magnification using a Nikon Diaphot microscope (Nikon Canada, Mississauga, ON, Canada) with a PixeLINK camera (PixeLINK, Ottawa, ON, Canada). Images were captured from at least two field views per plate. Branch points were counted for each treatment and plotted graphically.

Cell Proliferation Assay

Cell proliferation was analyzed colorimetrically by quantifying cleavage of WST-1 (Roche Diagnostics) by mitochondrial enzymes. Transfected HRECs were seeded at density of 2×10^4 cells per well in 96-well plates and cultured overnight. Cells were serum starved and treated with various glucose levels for 48 hours. At the end of the time point, 20 μL WST-1 was added to each well and incubated for 1 hour at 37°C. Absorbance was measured at 490 nm.[39]

Fluorescence In Situ Hybridization

Cells were seeded at 75% confluency in 12-well plates and treated with various glucose levels for 48 hours. Fluorescence in situ hybridization (FISH) was performed according to the manufacturer's protocol (biosearchtech.com/ stellaris protocols).[40] The probes were custom designed using the Stellaris

Investigative Ophthalmology & Visual Science

FISH probe designer and tagged with Cal Fluor Red 610 Dye (Biosearch Technologies, Petaluma, CA, USA). Following hybridization of probes, the cells were counterstained with Hoechst and mounted with Vectashield mounting medium (Vector Labs, Burligame, CA, USA). Positive stains were detected with a fluorescent microscope (Olympus BX51; Olympus, Richmond Hill, ON, Canada) and analyzed with ImageJ software (National Institutes of Health, Bethesda, MD, USA).

RNA Immunoprecipitation

The RNA immunoprecipitation (RIP) assay was conducted using the Magna RIP RNA-Binding Protein Immunoprecipitation Kit (Millipore, Etobicoke, ON, Canada) following the manufacturer's instruction.[41] Anti- EZH2 or anti-p300/CBP antibodies and IgG (control) were used for RIP (Millipore). Coprecipitated RNAs were detected with real time RT-PCR.

Immunohistochemistry

Mouse retinal sections were immunocytochemically stained for IgG using anti-mouse IgG antibody (MP Biomedicals, Solon, OH, USA) as previously described.[42] The stains were arbitrarily scored (0–3) in a masked fashion.

Statistical Analysis

Data are expressed as mean ± SEM. To determine statistical significance, 1-way ANOVA followed by Tukey's post hoc test was performed as appropriate, using fixed-level testing with a level of significance set at 5%. GraphPad Prism 5 (GraphPad, San Diego, CA, USA) software was used for statistical analysis.

Results

Glucose Regulates ANRIL Expression

The primary aim of this study was to identify the roles of glucose-induced alterations in lncRNA, to mediate gene transcription in the pathogenesis of diabetic retinopathy. As endothelial cells are primary targets of glucose-induced damage, we used these cells to perform our in vitro studies. Vascular endothelial growth factor is reported here as a downstream molecule that is regulated by ANRIL. Hence, HRECs were used to investigate alterations in ANRIL expression and its effect on VEGF expression and function. Human retinal endothelial cells were exposed to 25 mM D-glucose (HG) environments for various time points, using 5 mM D-glucose (NG) glucose levels as controls. We observed HG induced elevation in VEGF expression in a time-dependent manner, with highest expression at 48 hours (data not shown). Hence, for subsequent expression analysis, 48-hour glucose incubation was used. Microarray analysis conducted on HRECs after 48-hour HG incubation showed a 2.5-fold elevation in ANRIL (Fig. 1A). The results were validated by real-time RT-PCR (Fig. 1B). A significant (≈1.8-fold) increase was seen with HG. Such relatively smaller increase may possibly be explained by relatively small sample size. However, no significant ANRIL alteration was seen following 25 mM L-glucose (osmotic control) incubation (Fig. 1B). We performed RNA FISH for ANRIL to examine its cellular distribution and to detect its subcellular localization. We used custom designed RNA FISH probes consisting of 34 complementary oligonucleotides, each 20 bases long and labeled with a 3′ end flurophore tag. This approach has been shown to be highly specific for RNA detection.[43] Glucose-induced upregulation of ANRIL expression was confirmed by this technique. No change in subcellular distribution was noted following incubation with HG (Figs. 1C, 1D). Interestingly, the cells showed both cytoplasmic and nuclear distribution of ANRIL, although predominately localized in an around the cytoplasmic side of the nuclear envelope (Fig. 1C).

ANRIL Regulates Glucose-Induced Expression and Function of VEGF

We then proceeded to investigate mechanisms and significance of glucose-induced ANRIL upregulation. ANRIL has been shown to interact with the PRC2 complex that regulates VEGF expression.[9,31] The role of ANRIL in VEGF regulation was explored by knocking down ANRIL levels using siRNAs in HRECs. We used two siRNAs. As both gave similar results, data from one are shown. VEGF upregulation at mRNA and protein levels is characteristic of exposure of ECs to high levels of glucose. Such upregulation was prevented following ANRIL siRNA transfection, showing a direct regulatory relationship (Figs. 2A, 2B). As a functional parameter, we examined VEGF-mediated angiogenesis using tube formation assays on HRECs. Glucose-induced increased tube formation was prevented by ANRIL silencing. In addition, such reduction in siANRIL-transfected cells was rescued on further incubation with VEGF (Figs. 2C, 2D). The WST-1 assay further revealed that cell proliferation was inhibited in siANRIL-transfected cells compared with scrambled controls. Meanwhile, rescue experiments showed that VEGF incubation increased the cell proliferative ability in ANRIL-transfected cells both in LG and HG (Fig. 2E).

Diabetes-Induced Retinal VEGF Upregulation and Function Are Prevented in the ANRILKO Mice

With goals to translate our findings and establish the observation in diabetic conditions, we used ANRILKO mouse models. Due to the uncharacterized ANRIL mouse RNA sequence, as per standard practice, its expression in mice was measured using p15 as a surrogate marker for ANRIL (Fig. 3B).[38] The wild-type and knockout animals following STZ induction were monitored for a period of 2 months. Diabetic mice demonstrated hyperglycemia (Fig. 3A), polyuria, glycosuria, and reduced body weight gain, which are distinctive of poorly controlled diabetes (data not shown). ANRILKO had no effect on these parameters except for urine volume. Urine findings are further being investigated and will be reported separately.

We examined retinal tissues from the diabetic and control animals and analyzed for ANRIL and VEGF expression. ANRIL upregulation was observed in the retina of wild-type diabetic animals. In addition, VEGF mRNA and protein levels were elevated in diabetes. All such changes were prevented in the ANRILKO diabetic animals (Figs. 3C, 3D).

We stained the retinal tissues for IgG. Extravasated IgG is a marker for increased permeability, a functional effect of VEGF.[45] Diabetes caused increased retinal microvascular permeability in wild-type diabetic animals (score 3, compared with score 0 in wild-type controls), which was prevented in the retina of diabetic ANRILKO mice (score 1; Fig. 3E). These observations suggested that ANRIL regulates VEGF expression and its functional consequences in diabetic retinopathy.

ANRIL Causes VEGF Upregulation Through PRC Complex

We carried out additional in vitro experiments to gain mechanistic insight of ANRIL's actions as seen above. We

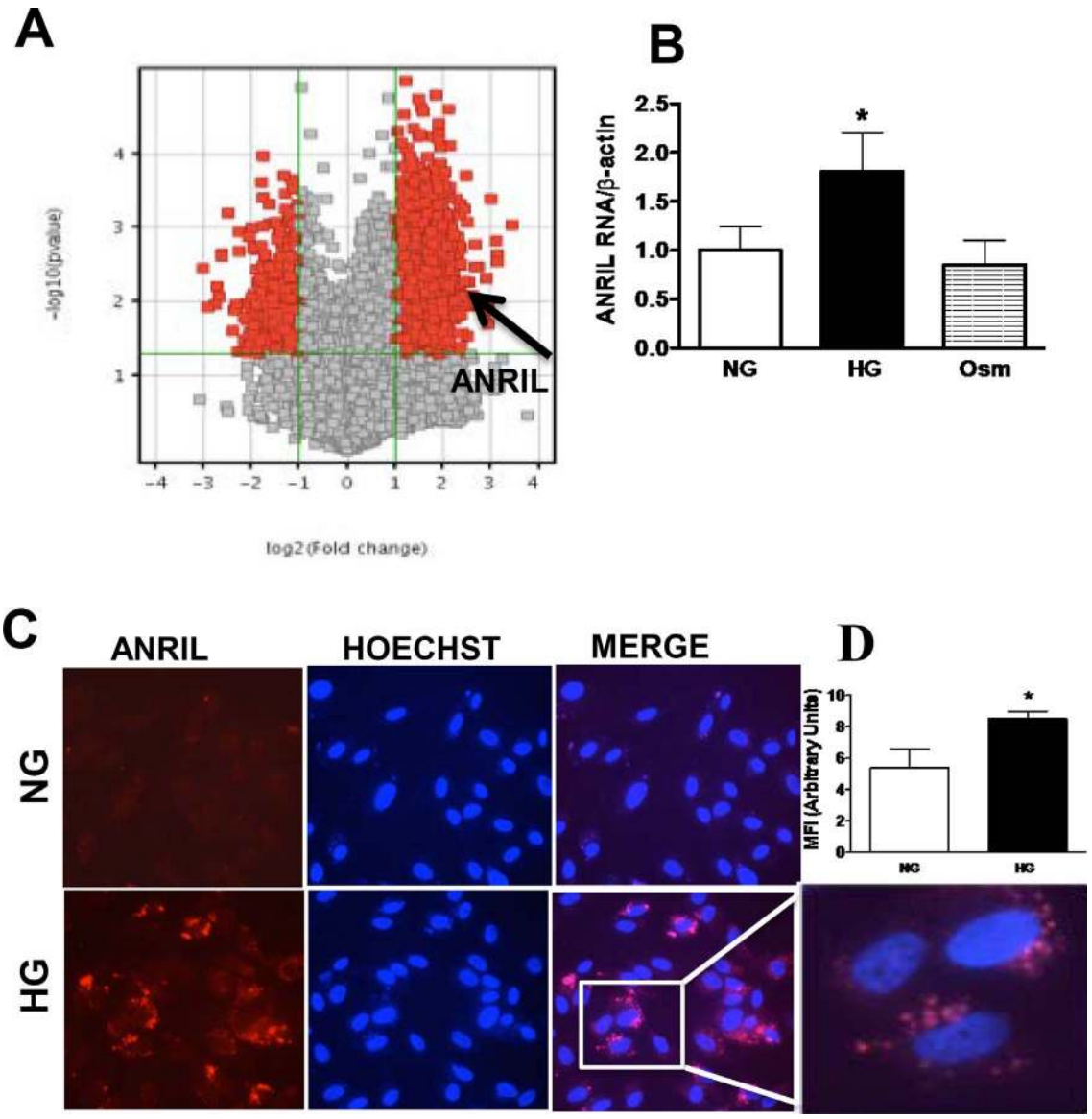

Figure 1. Alteration of lncRNA ANRIL in HG (25 mM) versus control (NG; 5 mM). (**A**) Volcano plot of differentially expressed lncRNAs in NG versus HG in HRECs. *Vertical lines* correspond to 1.2-fold changes up and down, respectively, and the *horizontal line* represents a *P* value of 0.05. *Red points* indicate differentially expressed genes with statistical significance. *Arrow* represents location of ANRIL. (**B**) Array data were validated by real-time RT-PCR analysis of ANRIL, which confirmed its increased expression on exposure to HG (48 hours). No alterations were seen following incubation with 25 mM L-glucose (osmotic control, Osm). (RNA expressions are presented as a ratio of β-actin, normalized to NG.) (**C**) Fluorescence in situ hybridization using probes against human ANRIL showed increased expression (nuclear and perinuclear cytoplasmic) in HRECs exposed to HG versus NG (48 hours). (**D**) Quantitative data following analysis using ImageJ confirmed glucose-induced ANRIL upregulation (MFI, mean fluorescence intensity). Images quantified by ImageJ (*$P < 0.05$ versus NG. $n = 4$ or more/group).

previously showed that glucose-induced miR200b-mediated VEGF upregulation works through the PRC2 complex.[9] PRC2 is part of transcriptional-repressive complexes PRCs (PRC1 and PRC2) and consists of many subunits (e.g., EZH2, EED, SUZ12, and RpAp46/48).[46] These complexes are critical in the epigenetic regulation of the CDKN2A/B locus.[31,47] Hence, we examined whether ANRIL has any regulatory relationship with the PRC2 complex in diabetic retinopathy. We measured expression of EZH2, which was upregulated in HRECs on exposure to HG, and in the retina of diabetic animals (Figs. 4A, 4D).[9] ANRILKO resulted in a significant downregulation of EZH2 levels (Figs. 4A, 4D). EED expression levels were similarly altered, whereas SUZ12 levels remained unaffected (Figs. 4B, 4C, 4E, 4F).

To establish a cause–effect relationship, we used DZNEP, a global methylase blocker, to inhibit PRC2 activity. All components of the PRC2 complex were suppressed by this methylase blocker (Figs. 4G–4I).[48] This blockade resulted in reduction of mRNA expression levels for both VEGF and ANRIL (Figs. 4J, 4K), suggesting a regulatory effect of PRC2 on ANRIL and VEGF.

ANRIL Acts Through p300 and miR200b

We have previously shown that VEGF is also regulated by miR200b through p300.[8] We explored the relationship of ANRIL in this context. Interestingly, we found that reduction in ANRIL expression using siRNA resulted in correction of glucose-induced upregulation of p300 (Fig. 5A). In retinal

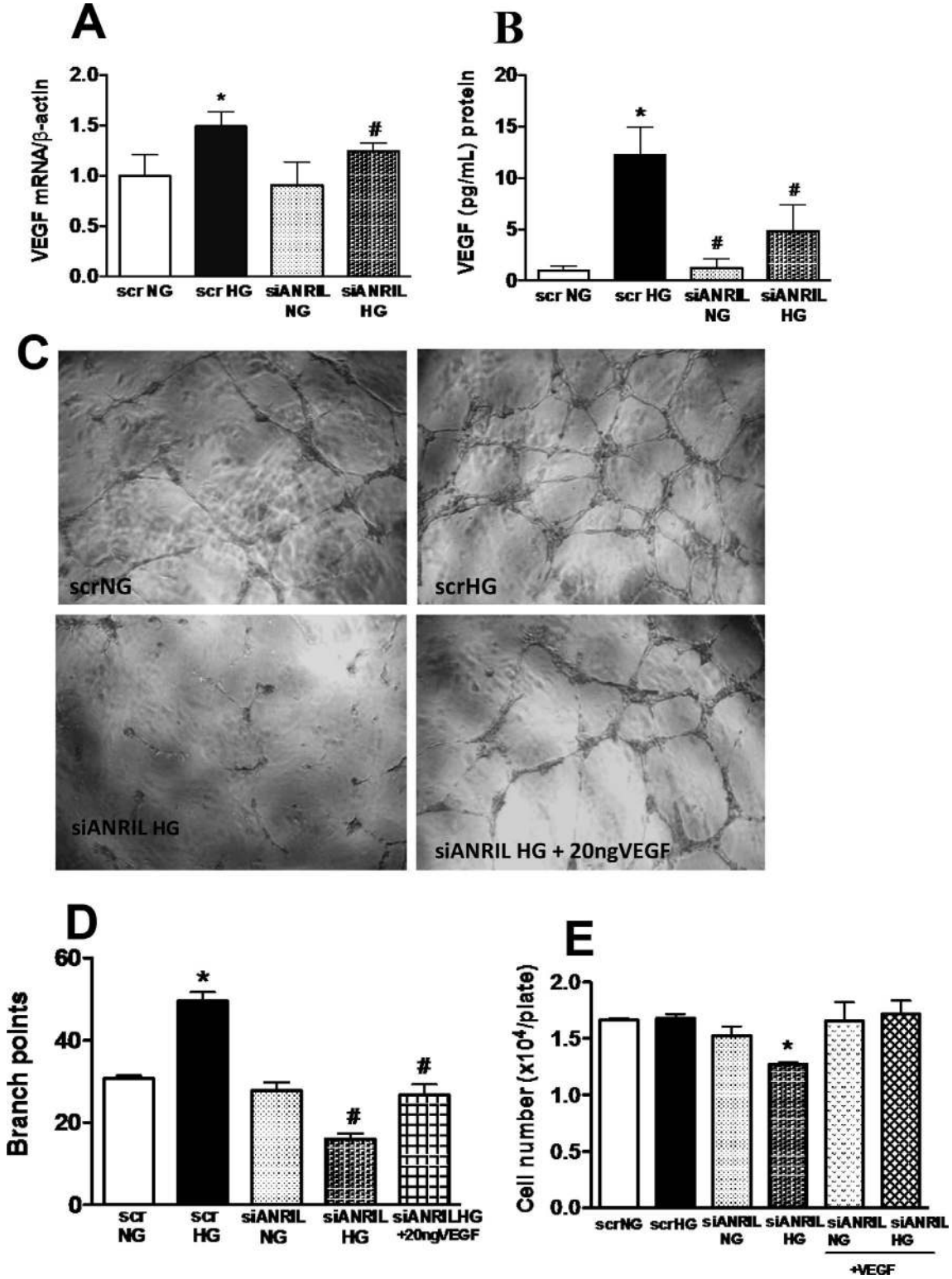

FIGURE 2. ANRIL regulates glucose-induced VEGF expression in HRECs (48 hours). Transfection of HRECs with ANRIL siRNA reduced (**A**) HG (25 mM glucose)-induced upregulation of VEGF mRNA and (**B**) protein expression compared with scrambled siRNA (scr). Endothelial tube formation assay shows (**C**) representative micrograph and (**D**) quantification using branch point assay. High glucose–induced increased endothelial tube formation was prevented by ANRIL siRNA, which was subsequently rescued by incubation with VEGF. (**E**) In parallel, ANRIL siRNA reduced endothelial cell proliferation (WST-1 assay), which was also reversed following VEGF incubation (NG = 5 mM glucose). Messenger RNA expressions are presented as a ratio of β-actin, normalized to NG. Protein levels are normalized to NG. $^{*,\#}P < 0.05$ versus scrNG or scrHG, $n = 4$ or more per group).

Investigative Ophthalmology & Visual Science

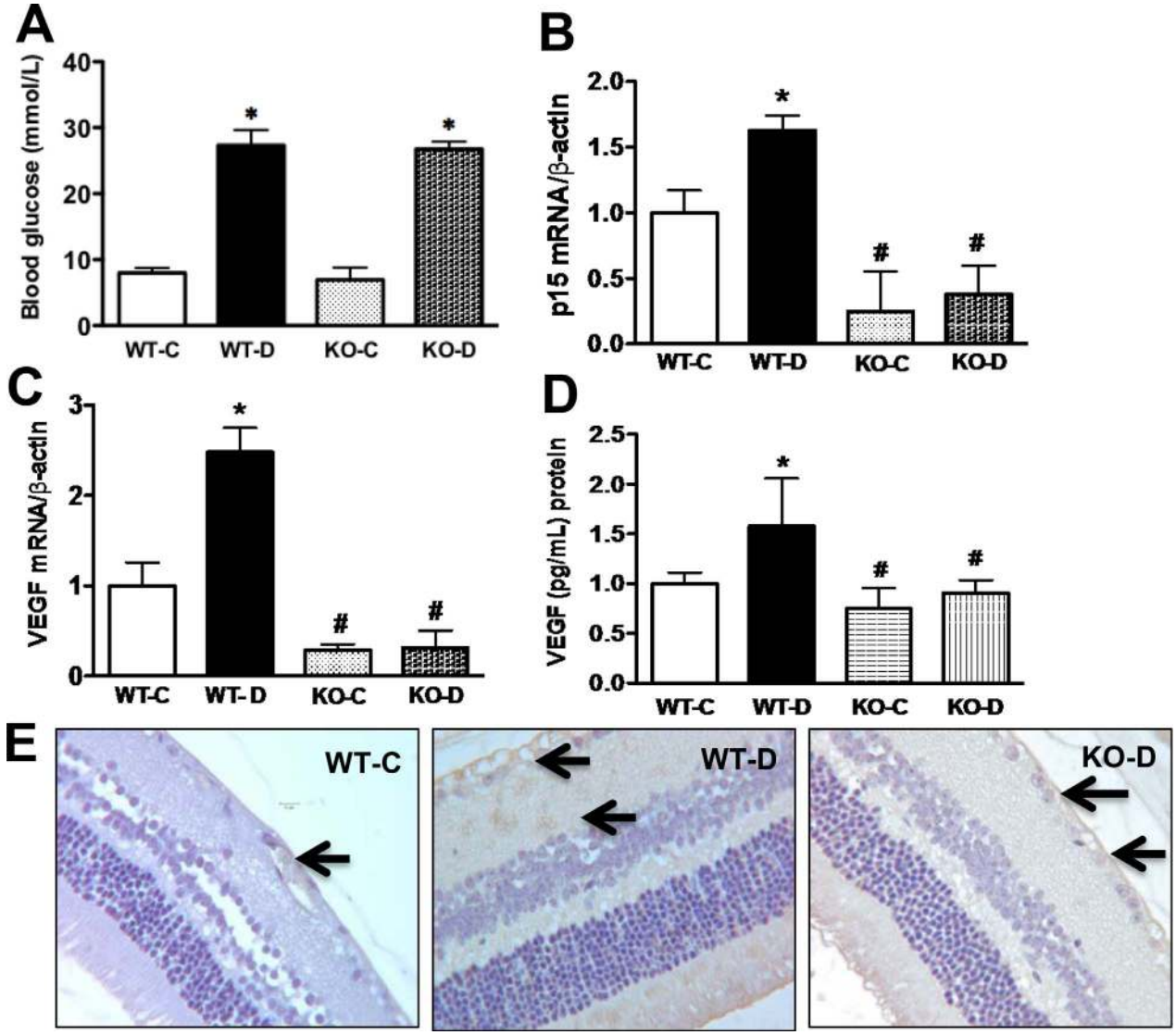

FIGURE 3. ANRIL regulates retinal VEGF in diabetic mice. (**A**) Diabetic wild-type (WT-D) mice and diabetic ANRILKO (KO-D) mice showed hypergylcemia and reduced body weight (data not shown). (**B**) Basal and diabetes-induced ANRIL RNA expression in the retina, measured by p15, its surrogate marker, was significantly reduced in the control ANRILKO mice (KO-C) mice and KO-D mice. Diabetes-induced elevation of VEGF (**C**) mRNA and (**D**) protein expression levels were also prevented in retina of KO-C and KO-D animals. (**E**) Immunohistochemical stain on mouse retina using anti-IgG antibody showing increased extravascular diffuse stain, indicating increased extravasation (score 3) in the WT-D compared with wild-type controls (WT-C) (score 0). Such changes were prevented in KO-D (score 1). Messenger RNA expressions are presented as a ratio of β-actin, normalized to WT-C. Protein levels are normalized to WT-C. $^{*,\#}P < 0.05$ versus WT-C or WT-D, $n = 8$.

tissues of control and diabetic animals, ANRILKO also significantly reduced expression of p300 (Fig. 5B). These findings indicate that ANRIL regulates glucose-mediated increase in p300 in diabetic retinopathy.[8,34] To further examine possible feedback regulation of ANRIL by p300, we silenced p300 in HRECs (such silencing led to ≈75% reduction in p300 mRNA expression) and observed no effect of this alteration on ANRIL expression (Fig. 5C). On the other hand, ANRIL silencing also reduced glucose-induced miR200b downregulation (Fig. 5D).

We further established possible interaction of ANRIL with EZH2 component of PRC2 and p300 thorough RNA-IP assay in HRECs. ANRIL expression levels were determined by real-time RT-PCR on the samples immunoprecipitated using specific antibodies to EZH2 and p300 (Figs. 5E, 5F). Binding of ANRIL to p300 was significantly elevated when exposed to high glucose levels. There was also increase in EZH2 binding to ANRIL under HG. These data strongly indicate that ANRIL directly binds to both p300 and EZH2 when exposed to high levels of glucose.

DISCUSSION

In this study, we demonstrated that lncRNA ANRIL is upregulated in response to high levels of glucose. ANRIL regulates glucose-mediated upregulation of VEGF through its interaction with p300 and PRC2 components in glucose-exposed ECs and in the retinal tissue of diabetic animals.

Present-day treatments for proliferative diabetic retinopathy revolve around destructive treatments of laser photocoagulation, vitreo-retinal surgery, and blocking VEGF signaling.[49] Targeting the transcriptional process may constitute a novel approach. The majority of human genome sequences studied until now are protein coding, which

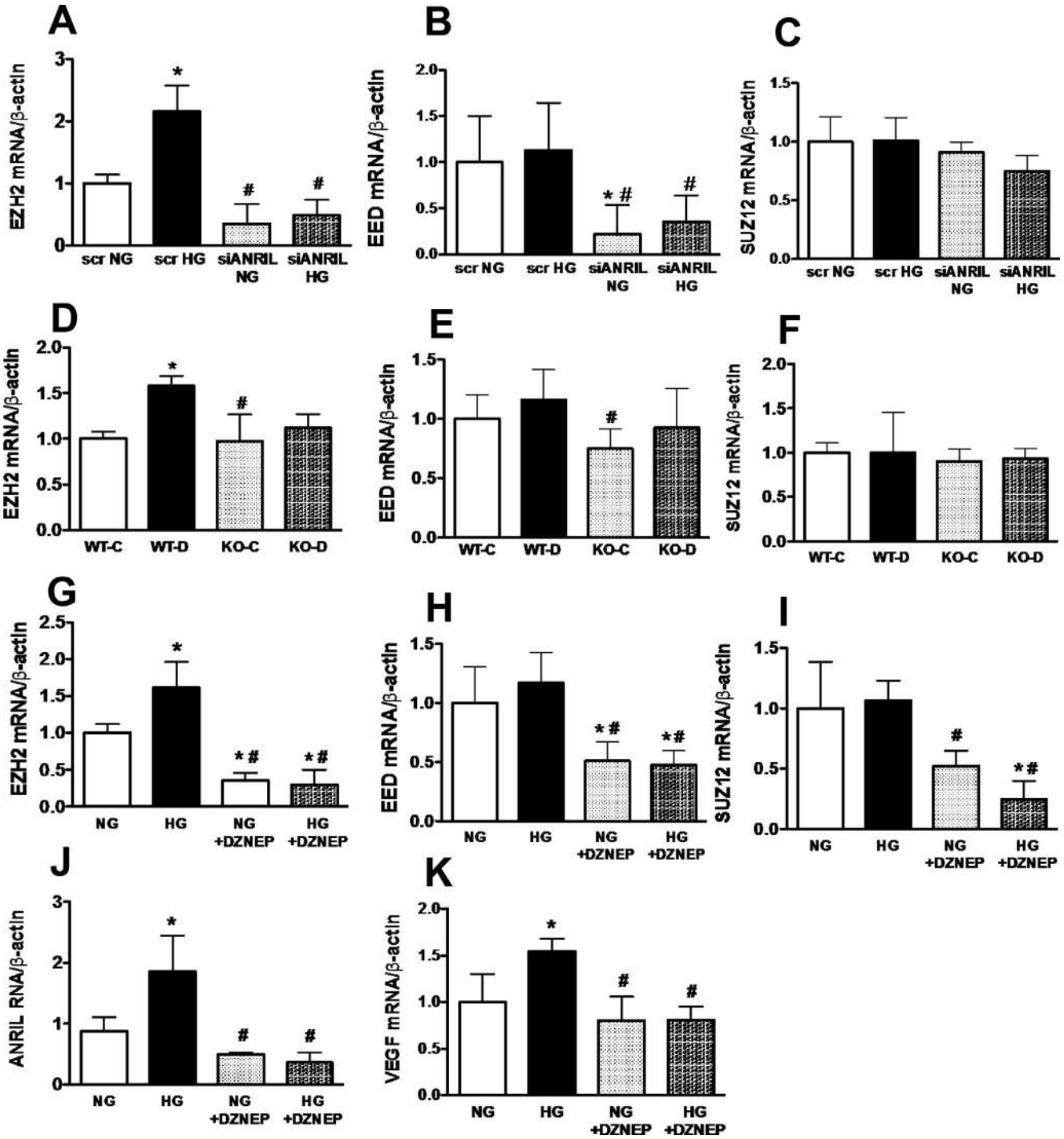

FIGURE 4. ANRIL–PRC2 complex interaction. Transfection of HRECs (48 hours) with siANRIL reduced HG (25 mM glucose)-induced (**A**, **B**) upregulation of EZH2 and EED mRNA, whereas SuZ12 mRNA (**C**) remained unaltered. (**D**–**F**) Diabetes-induced increased retinal mRNA expression of EZH2 and EED was similarly reduced in ANRILKO mice [controls (KO-C) and diabetic (KO-D)], whereas SUZ12 levels were unaffected. (**G**) EZH2 mRNA overexpression in HG were blocked by the global histone methylation inhibitor DZNEP. (**H**, **I**) 3-Deazaneplanocin A also reduced upregulation of EED and SUZ12. (**J**, **K**) 3-Deazaneplanocin A also reduced glucose-induced ANRIL and VEGF mRNA upregulation (WT-C, WT-D, NG [5 mM glucose]). Messenger RNA expressions are presented as a ratio of β-actin, normalized to NG/WT-C. $^{*}P < 0.05$ versus scrNG/WT-C, $^{\#}P < 0.05$ versus scrHG or WT-D, and $n = 8$ or more per group.

comprises only 1.5% of the entire genome.[50] Recently, focus has been drawn onto the remaining noncoding area of the genome and its importance in normal development and relevance in diseases.[51] Noncoding RNAs generated from noncoding areas, when functional, exerts regulatory activities independent of the protein-encoding route. Hence, they constitute potential drug targets.[52] Here we focus on a specific lncRNA in diabetic retinopathy.

The various roles of lncRNAs include modulation of alternate splicing, chromatin remodeling, *cis/trans*-acting regulators of gene expression, and RNA metabolism.[53–56] Dysregulation of target genes leads to abnormal lncRNA

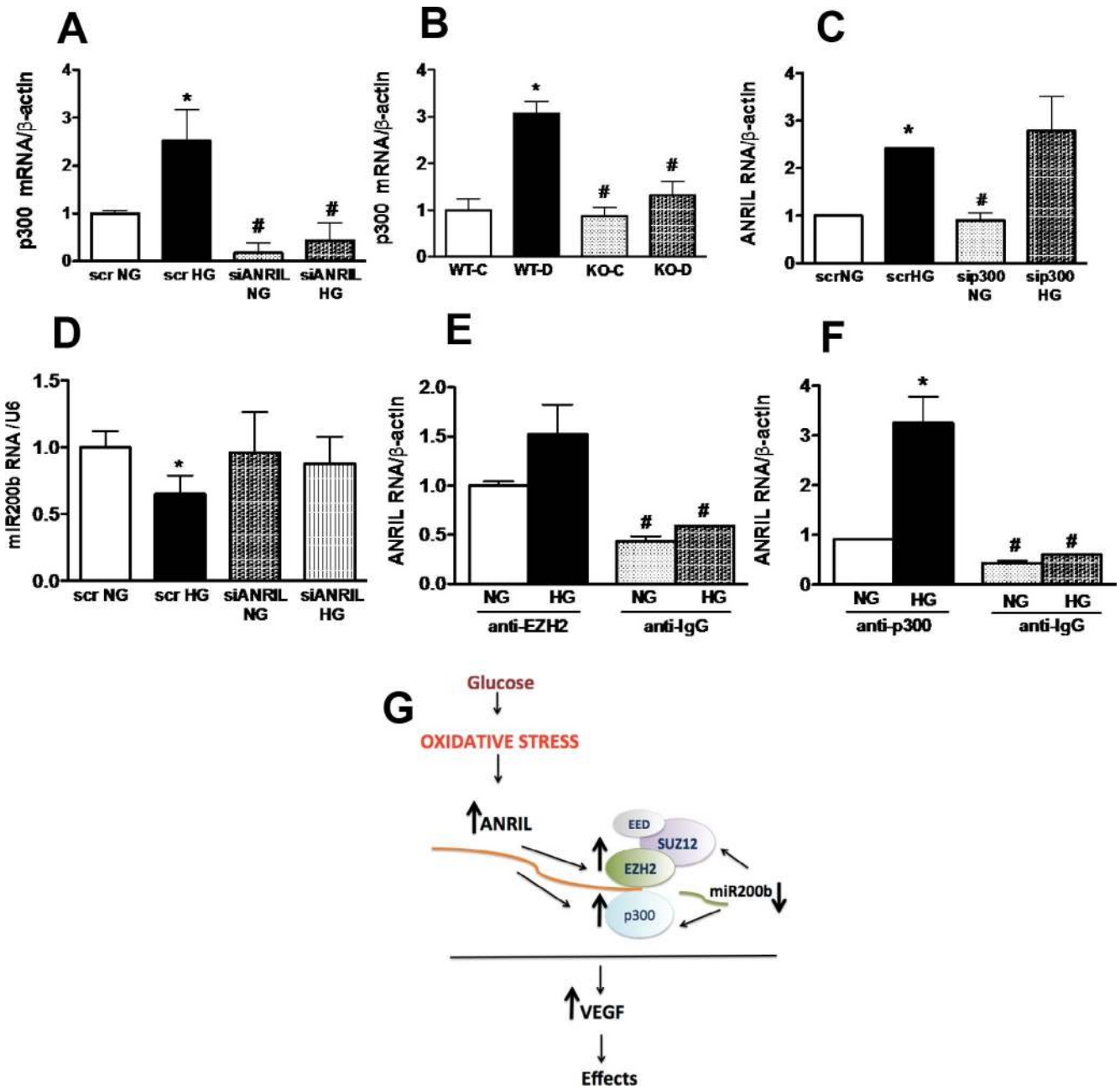

FIGURE 5. Interaction of ANRIL with the histone acetylator p300 and miR200b.Transfection of HRECs (48 hours) with siANRIL reduced HG (25 mM glucose)-induced (**A**) upregulation of p300 and (**D**) downregulation of miR200b versus control (NG; 5 mM glucose). (**B**) Diabetes-induced elevated p300 mRNA expressions were prevented in the retinal tissues of diabetic ANRILKO mice (KO-D; $n = 8$/group). (**C**) However, silencing of p300 by siRNA did not alter ANRIL mRNA expression in HRECs. (**E**, **F**) RNA-IP with anti-EZH2 and anti-p300 performed in HRECs showed glucose-induced increased binding of ANRIL with the molecules (anti-IgG as negative control). (**G**) A schematic outline of the mechanism related to ANRIL upregulation and its interactions with p300,miR200b and PRC2 complex in mediating VEGF upregulation in diabetic retinopathy (WT-C, WT-D, KO-C). Messenger RNA expressions are presented as a ratio of β-actin, normalized to NG/WT-C. $^{*}P < 0.05$ versus WT-C or scrNG or anti-p300NG, $^{\#}P < 0.05$ versus WT-D or scrHG or anti-EZH2HG or anti-p300HG. $n = 3$ or more per group of cells.

expression responsible for cellular defects and disease progression including carcinogenesis and neurodegeneration.[51,57] Our study demonstrates an important and novel regulatory role of lncRNA ANRIL in VEGF regulation in diabetic retinopathy.

Originally identified from familial melanoma patients, ANRIL is a potential target for cardiovascular diseases.[24] It has been known to be associated with diabetes, open angle glaucoma, and various cancers.[58] We found that ANRIL binds to both p300 and EZH2 of the PRC2 complex to regulate VEGF expression, characteristic of retinal degeneration in diabetes. Microarray analysis followed by cellular and tissue data confirmed the glucose-mediated upregulation of ANRIL. Interestingly, ANRIL showed perinuclear localization in HRECs. In contrast, ANRIL has been previously reported to show nuclear expression in gastric cancer.[33] However, lncRNAs have been observed to show cell-to-cell variability in expression patterns.[59]

Histone methylation and acetylation are well-characterized epigenetic marks implicated in diabetic complications.[60,61]

Histone methylation involves transfer of methyl groups to amino acid residues by histone methyltransferases such as EZH2 (PRC2 complex).[62] In some tumors, increased EZH2 promotes VEGF stimulation and subsequent angiogenesis.[63] In our experiments, in ANRIL-silenced HRECs and in ANRILKO mice, reduced levels of VEGF were accompanied by EZH2 reduction. EZH2 blockade resulted in reduction in ANRIL and VEGF RNA expression, showing a cause–effect relationship. We previously demonstrated the interaction of miR200b with SUZ12 of the PRC2 complex in the regulation of VEGF.[9] The upregulation of miR200b in siANRIL-transfected HRECs suggests another interaction of ANRIL with mir200b in the regulation of VEGF.

Diabetic ANRILKO animals and HRECs in HG following ANRIL siRNA transfection showed reduction in p300 mRNA expression. We previously demonstrated that p300 is upregulated in diabetes and it controls multiple gene expressions.[64] We have previously shown miR200b-dependent increased production of p300 in diabetic retinopathy,[8] and that glucose-induced upregulation of VEGF was prevented by p300siRNA.[34] Retinal tissues from ANRILKO diabetic animals showed downregulated expression of p300 along with the lowering of VEGF. Furthermore, the RNA-IP assay revealed significantly stronger binding of ANRIL with p300 after exposure to HG. Hence, another route of ANRIL regulating VEGF may be mediated through its effect on the transcriptional regulator, p300. To the best of our knowledge, this is also the first direct demonstration of ANRIL-mediated p300 regulation in diabetes. A schematic of the regulatory process as observed in this study is outlined in Figure 5G.

Numerous lncRNAs associate with and possibly target histone-modifying activities.[59] Long ncRNA scaffolds are now known to organize the concerted activities of chromatin-modifying complexes spatially and temporally.[65,66] For example, HOX transcript antisense RNA (HOTAIR) associates with PRC2 and Lys-specific demethylase 1 (LSD1).[67] PRC2 and LSD1 are responsible for the deposition of the repressive histone marks and removal of active histone marks, respectively. Recently, in other systems, overexpression of ANRIL is known to change p300, mediating epigenetic modifications.[32] Hence, a pattern of combined interaction of ANRIL with PRC2 and p300 might be an important mechanism in its regulation of VEGF in diabetic retinopathy. Hence, ANRIL-mediated VEGF upregulation is not direct and is mediated by the aforesaid molecules. However, it is possible that additional molecules, including other lncRNAs and other mediators, may potentially be involved in such regulations. Such pathways need additional investigation.

Although there are no previous reports on ANRIL alterations in diabetic retinopathy, recently another lncRNA myocardial infarction associated transcript (MIAT) has been shown to be upregulated in diabetic retinopathy.[68] However, exact pathways for ANRIL upregulation in the genome are not clear. Long ncRNAs are under the same regulatory process as that of coding genes.[69] Hence, hyperglycemia-induced oxidative stress and subsequent alterations of transcriptional machinery may also potentially regulate such process.

In summary, we showed that, in the retinal endothelial cells, glucose causes upregulation of ANRIL. This upregulation is responsible for altered VEGF expression and function. We further confirmed these novel findings in ANRILKO mice with STZ-induced diabetes. The regulatory effect of ANRIL on VEGF was mediated by interactions of ANRIL with components of the PRC2 complex and the histone acetylator p300. The current data from this study shed light on a potentially new, targeted method to prevent diabetic retinopathy using an RNA-based approach.

Acknowledgments

Supported by grants from the Canadian Diabetes Association.

Disclosure: **A.A. Thomas**, None; **B. Feng**, None; **S. Chakrabarti**, None

References

1. Lingam G, Wong TY. Systemic medical management of diabetic retinopathy. *Middle East Afr J Ophthalmol*. 2013; 20:301–308.
2. Adamis AP. Is diabetic retinopathy an inflammatory disease? *Br J Ophthalmol*. 2002;86:363–365.
3. Lutty GA. Effects of diabetes on the eye. *Invest Ophthalmol Vis Sci*. 2013;54:81–87.
4. Cade WT. Diabetes-related microvascular and macrovascular diseases in the physical therapy setting. *Phys Ther*. 2008;88: 1322–1335.
5. Carmeliet P. Angiogenesis in life, disease and medicine. *Nature*. 2005;438:932–936.
6. Ferrara N, Gerber HP, LeCouter J. The biology of VEGF and its receptors. *Nat Med*. 2003;9:669–676.
7. Wirostko B, Wong TY, Simo R. Vascular endothelial growth factor and diabetic complications. *Prog Retin Eye Res*. 2008; 27:608–621.
8. McArthur K, Feng B, Wu Y, Chen S, Chakrabarti S. MicroRNA-200b regulates vascular endothelial growth factor-mediated alterations in diabetic retinopathy. *Diabetes*. 2011;60:1314–1323.
9. Ruiz M, Feng B, Chakrabarti S. Polycomb repressive complex 2 regulates MiR-200b in retinal endothelial cells: potential relevance in diabetic retinopathy. *PLoS One*. 2015;10:1–21.
10. Haque R, Hur EH, Farrell AN, Iuvone M, Howell JC. MicroRNA-152 represses VEGF and TGFβ1 expressions through post-transcriptional inhibition of (Pro)renin receptor in human retinal endothelial cells. *Mol Vis*. 2015;21:224–235.
11. Portela A, Esteller M. Epigenetic modifications and human disease. *Nat Biotechnol*. 2010;28:1057–1068.
12. Sharma S, Kelly TK, Jones PA. Epigenetics in cancer. *Carcinogenesis*. 2010;31:27–36.
13. Ambros V. The functions of animal microRNAs. *Nature*. 2004; 431:350–355.
14. Bushati N, Cohen SM. microRNA functions. *Annu Rev Cell Dev Biol*. 2007;23:175–205.
15. Mercer TR, Dinger ME, Mattick JS. Long non-coding RNAs: insights into functions. *Nat Rev Genet*. 2009;10:155–159.
16. Wilusz JE, Sunwoo H, Spector DL. Long noncoding RNAs: functional surprises from the RNA world. *Genes Dev*. 2009; 23:1494–1504.
17. Wapinski O, Chang HY. Long noncoding RNAs and human disease. *Trends Cell Biol*. 2011;21:354–361.
18. Isin M, Dalay N. LncRNAs and neoplasia. *Clin Chim Acta*. 2015;444:280–288.
19. Yang G, Lu X, Yuan L. LncRNA: a link between RNA and cancer. *Biochim Biophys Acta*. 2014;1839:1097–1109.
20. Guffanti A, Simchovitz A, Soreq H. Emerging bioinformatics approaches for analysis of NGS-derived coding and non-coding RNAs in neurodegenerative diseases. *Front Cell Neurosci*. 2014;8:1–10.
21. Soreq L, Guffanti A, Salomonis N, et al. Long non-coding RNA and alternative splicing modulations in Parkinson's leukocytes identified by RNA sequencing. *PLoS Comput Biol*. 2014;10:1–22.
22. Cabianca DS, Casa V, Bodega B, et al. A long ncRNA links copy number variation to a polycomb/trithorax epigenetic switch in FSHD muscular dystrophy. *Cell*. 2012;149:819–831.

23. Van Dijk M, Thulluru HK, Mulders J, et al. HELLP babies link a novel lincRNA to the trophoblast cell cycle. *J Clin Invest*. 2012;122:4003–4011.
24. Companioni O, Rodríguez FE, Fernández-Aceituno M, Rodriguez Pérez JC. Genetic variants, cardiovascular risk and genome-wide association studies. *Rev Esp Cardiol*. 2011;64: 509–514.
25. Broadbent HM, Peden JF, Lorkowski S, et al. Susceptibility to coronary artery disease and diabetes is encoded by distinct, tightly linked, SNPs in the ANRIL locus on chromosome 9p. *Hum Mol Genet*. 2008;17:806–814.
26. Cugino D, Gianfagna F, Santimone I, et al. Type 2 diabetes and polymorphisms on chromosome 9p21: a meta-analysis. *Nutr Metab Cardiovasc Dis*. 2012;22:619–625.
27. Burdon KP, Macgregor S, Hewitt AW, et al. Genome-wide association study identifies susceptibility loci for open angle glaucoma at TMCO1 and CDKN2BAS1. *Nat Genet*. 2011;43: 574–578.
28. Pasmant E, Sabbagh A, Vidaud M, Bieche I. ANRIL, a long, noncoding RNA, is an unexpected major hotspot in GWAS. *FASEB J*. 2011;25:444–448.
29. Cunnington MS, Santibanez Koref M, Mayosi BM, Burn J, Keavney B. Chromosome 9p21 SNPs associated with multiple disease phenotypes correlate with ANRIL expression. *PLoS Genet*. 2010;6:1–17.
30. Bochenek G, Hasler R, El Mokhtari N, et al. The large noncoding RNA ANRIL, which is associated with atherosclerosis, periodontitis and several forms of cancer, regulates ADIPOR1, VAMP3 and C11ORF10. *Hum Mol Genet*. 2013;22:4516–4527.
31. Popov N, Gil J. Epigenetic regulation of the INK4b-ARF-INK4a locus: in sickness and in health. *Epigenetics*. 2010;5:685–690.
32. Sato K, Nakagawa H, Tajima A, Yoshida K, Inoue I. ANRIL is implicated in the regulation of nucleus and potential transcriptional target of E2F1. *Oncol Rep*. 2010;24:701–707.
33. Zhang EB, Kong R, Yin DD, et al. Long noncoding RNA ANRIL indicates a poor prognosis of gastric cancer and promotes tumor growth by epigenetically silencing of miR-99a/miR-449a. *Oncotarget*. 2014;5:2276–2292.
34. Chen S, Feng B, George B, Chakrabarti R, Chen M, Chakrabarti S. Transcriptional coactivator p300 regulates glucose-induced gene expression in endothelial cells. *Am J Physiol Endocrinol Metab*. 2010;298:E127–E137.
35. Gray MJ, Zhang J, Ellis LM, et al. HIF-1alpha, STAT3, CBP/p300 and Ref-1/APE are components of a transcriptional complex that regulates Src-dependent hypoxia-induced expression of VEGF in pancreatic and prostate carcinomas. *Oncogene*. 2005;24:3110–3120.
36. Kantharidis P, Wang B, Carew RM, Lan HY. Diabetes complications: the microRNA perspective. *Diabetes*. 2011; 60:1832–1837.
37. Feng B, Cao Y, Chen S, Ruiz M, Chakrabarti S. miRNA-1 regulates endothelin-1 in diabetes. *Life Sci*. 2014;98:18–23.
38. Visel A, Zhu Y, May D, et al. Targeted deletion of the 9p21 non-coding coronary artery disease risk interval in mice. *Nature*. 2010;464:409–412.
39. Khalife R, El-Hayek S, Tarras O, Hodroj MH, Rizk S. Antiproliferative ad proapoptotic effects of topotecan in combination with thymoquione on acute myelogenous leukemia. *Clin Lymphoma Myleoma Leuk*. 2014;14:S46–S55.
40. Zhang X, Li H, Burnett JC, Rossi JJ. The role of antisense long noncoding RNA in small RNA-triggered gene activation. *RNA*. 2014;20:1916–1928.
41. Huang MD, Chen WM, Qi FZ, et al. Long non-coding RNA ANRIL is upregulated in hepatocellular carcinoma and regulates cell apoptosis by epigenetic silencing of KLF2. *J Hematol Oncol*. 2015;8:1–14.
42. Cukiernik M, Hileeto D, Evans T, Mukherjee S, Downey D, Chakrabarti S. Vascular endothelial growth factor in diabetes induced early retinal abnormalities. *Diabetes Res Clin Pract*. 2004;65:197–208.
43. Raj A, van den Bogaard P, Rifkin SA, van Oudenaarden A, Tyagi S. Imaging individual mRNA molecules using multiple singly labeled probes. *Nat Methods*. 2008;5:877–879.
44. Aguilo F, Zhou MM, Walsh MJ. Long noncoding RNA, polycomb, and the ghosts hauting INK4b-ARF-INK4a expression. *Cancer Res*. 2011;71:5365–5369.
45. Hofman P, Blaauwgeers HG, Tolentino MJ, et al. VEGF-A induced hyperpermeability of blood-retinal barrier endothelium in vivo is predominantly associated with pinocytotic vesicular transport and not with formation of fenestrations. Vascular endothelial growth factor-A. *Curr Eye Res*. 2000;2: 637–645.
46. Di Croce L, Helin K. Transcriptional regulation by Polycomb group proteins. *Nat Struct Mol Biol*. 2013;20:1147–1155.
47. Kia SK, Gorski MM, Giannakopoulos S, Verrijzer CP. SWI/SNF mediates polycomb eviction and epigenetic reprogramming of the INK4b-ARF-INK4a locus. *Mol Cell Biol*. 2008;28:3457–3464.
48. Tan J, Yang X, Zhuang L, et al. Pharmacologic disruption of polycomb-repressive complex 2-mediated gene repression selectively induces apoptosis in cancer cells *Genes & Dev*. 2007;21:1050–1063.
49. Mohamed Q, Gillies MC, Wong TY. Management of diabetic retinopathy—a systematic review. *J Am Med Assoc*. 2007;298: 902–916.
50. Alexander RP, Fang G, Rozowsky J, Snyder M, Gerstein MB. Annotating non-coding regions of the genome. *Nature Rev Gen*. 2010;11:559–571.
51. Esteller M. Non-coding RNAs in human disease. *Nature Rev Genet*. 2011;12:861–874.
52. Wahlestedt C. Natural antisense and noncoding RNA transcripts as potential drug targets. *Drug Discov Today*. 2006;11: 503–508.
53. Gutschner T, Diederichs S. The hallmarks of cancer: a long non-coding RNA point of view. *RNA Biol*. 2012;9:703–719.
54. Gupta RA, Shah N, Wang KC, et al. Long non-coding RNA HOTAIR reprograms chromatin state to promote cancer metastasis. *Nature*. 2010;464:1071–1076.
55. Kotake Y, Nakagawa T, Kitagawa K, et al. Long non-coding RNA ANRIL is required for the PRC2 recruitment to and silencing of p15(INK4B) tumor suppressor gene. *Oncogene*. 2011;30:1956–1962.
56. Nagano T, Fraser P. No-nonsense functions for long noncoding RNAs. *Cell*. 2011;145:178–181.
57. Salta E, De Strooper B. Non-coding RNAs with essential roles in neurodegenerative disorders. *Lancet Neurol*. 2012;11:189–200.
58. Congrains A, Kamide K, Ohishi M, Rakugi H. ANRIL: molecular mechanisms and implications in human health. *Int J Mol Sci*. 2013;14:1278–1292.
59. Cabili MN, Dunagin MC, McClanahan PD, et al. Localization and abundance analysis of human lncRNAs at single-cell and single-moleucle resolution. *Genome Biol*. 2015;16:1–16.
60. Villeneuve LM, Natarajan R. The role of epigenetics in the pathology of diabetic complications. *Am J Physiol Renal Physiol*. 2010;299:F14–F25.
61. Pirola L, Balcerczyk A, Okabe J, El-Osta A. Epigenetic phenomena linked to diabetic complications. *Nat Rev Endocrinol*. 2010;6:665–675.
62. Byvoet P, Shepherd GR, Hardin JM, Noland BJ. The distribution and turnover of labeled methyl groups in histone fractions of cultured mammalian cells. *Arch Biochem Biophys*. 1972;148:558–567.

Investigative Ophthalmology & Visual Science

63. Chang CJ, Hung MC. The role of EZH2 in tumor progression. *Br J Cancer*. 2012;106:243–247.
64. Feng B, Chen S, Chiu J, George B, Chakrabarti S. Regulation of cardiomyocyte hypertrophy in diabetes at the transcriptional level. *Am J Physiol Endocrinol Metab*. 2008;294:E1119–E1126.
65. Kugel JF, Goodrich JA. Non-coding RNAs: key regulators of mammalian transcription. *Trends Biochem Sci*. 2012;37:144–151.
66. Spitale, RC, Tsai MC, Chang HY. RNA templating the epigenome: long noncoding RNAs as molecular scaffolds. *Epigenetics*. 2011;6:539–543.
67. Tsai MC, Manor O, Wan Y, et al. Long noncoding RNA as modular scaffold of histone modification complexes. *Science*. 2010;329:689–693.
68. Jaé N, Dimmeler S. Long noncoding RNAs in diabetic retinopathy. *Circ Res*. 2015;116:1104–1106.
69. Wu Z, Liu X, Liu L, et al. Regulation of lncRNA expression. *Cell Mol Biol Lett*. 2014;19:561–575.

Investigative Ophthalmology & Visual Science